Conformational Study of Silklike Peptides Modified by the Addition of the Calcium-Binding Sequence from the Shell Nacreous Matrix Protein MSI60 Using ^{13}C CP/MAS NMR Spectroscopy

Tetsuo Asakura,*,† Megumi Hamada,† Sung-Won Ha,† and David P. Knight‡

Department of Biotechnology and Life Science, Tokyo University of Agriculture and Technology, Koganei, Tokyo 184-8588, Japan, and Oxford Biomaterials Ltd., Units 14-15 Galaxy House, Thatcham RG19 6HR, U.K.

Received February 20, 2006; Revised Manuscript Received April 3, 2006

The calcium-binding site of the pearl oyster (*Pinctada fucata*) nacreous layer matrix protein MSI60 was introduced between different Ala-Gly repeating regions derived from the primary sequences of several silk fibroins. Several different organic solvents whose effect on the repetitive domains of silk peptides is well-understood were used to modify the secondary structure of the flanking Ala-Gly repeating regions. The local conformations of the flanking Ala-Gly repeating regions as well as the calcium-binding motif, MSI60, were determined by ^{13}C CP/MAS NMR spectroscopy. The secondary structures of the polyalanine, poly(Ala), domains were modified by the solvent treatments in a predictable fashion, suggesting that only the solvent treatment and not the conformation of the MSI60 domain affected the conformation of poly(Ala) regions. Ala-Gly domains behaved differently, taking random coil conformation regardless of the choice of solvent, indicating that their secondary structure is affected by the central MSI60 domain. The conformation of the MSI60 domain is not altered by the solvent treatments, suggesting that it may retain its ability to bind calcium ions. This was confirmed using a calcium-binding assay. The assay further showed that the calcium-binding capability of MSI60 in the synthetic peptides was most effective when the flanking domain was in the β-sheet structure.

Introduction

Silks from different species have their own unique amino acid compositions and primary sequences (Figure 1).[1,2] For instance, the repetitive primary sequences in *Bombyx mori* (*B. mori*) are dominated by iterations of a GAGAGS motif,[3,4] while blocks of poly(Ala) separated by glycine-rich blocks make up the repetitive structure in *Antheraea pernyi* (*A. pernyi*)[5] and *Antheraea yamamai* (*A. yamamai*)[6] cocoon silk fibroin and *Nephila clavipes* (*N. clavipes*) dragline silk spidroins, MaSp1 and MaSp2.[7] Highly ordered β-sheet crystals oriented along the fiber axis contribute to the excellent mechanical properties of silks. This creates an expectation that silks could be extremely useful as strong and tough implantable biomaterials and scaffolds for tissue engineering[1]. The fact that natural silk fibroins are capable of mineralization with the bone mineral hydroxyapatite[8,9] suggests that they may have potential use as bone graft substitute materials. This, and an earlier study,[10] was motivated by the possibility that modification of silk sequence by including calcium-binding domains from other proteins may improve mineralization.

Accordingly, in the present study, we aimed to produce synthetic silklike peptides containing the calcium-binding domain of the MSI60 found in the nacreous layer of pearl oyster, *Pinctada fucata*,[11] and test their ability to bind calcium ions. MSI60 is one of the matrix proteins present in the nacreous layer of the shell where it lies between the crystalline layers of aragonite, one of the crystalline forms of $CaCO_3$. These matrix proteins regulate the epitaxial growth and thickness of the aragonite crystals and thus help to produce the extremely tough multilaminate structure of the shell nacre.[12,13] Few structural studies of the proteins in the nacreous layer have been done

A. pernyi
AAAAAAAAAAAAA GSGAGGSGGYGGYGGYGSDS
AAAAAAAAAAAAA GSSAGGAGGGYGWGDGGYGSDS
AAAAAAAAAAAAA GSGAGGSGGYGGYGSDS
AAAAAAAAAAAAA GSSAGGAGGGYGWGDGGYGSDS
AAAAAAAAAAAA SSGAGGRGDGGYGSGGSS

B. mori
GAGAGSGAAFGAGAGAGAGSGAGAGSGAGAGSGAGAGSGAGAG
SGAGAGYGAGYGAGVGAGYGAGAGSGAASGAGAGSGAGAGSGA
GAGSGAGAGSGAGAGSGAGAGYGAGVGAGYGAGYGAGAGAGY
GAGAGSGAASGAGAGSGAGAGAGSGAGAGSGAGAGSGAGAGS
GAGSGAGAGSGAGAGSGAGAGYGAGAGSGAASGAGAGAGA

N. clavipes
AAAAAA GGAGQGGYGGLGGQGAGQGGYGGLGGQGAGQGAG
AAAAAAA GGAGQGGYGGLGSQGAGRGGQGAG
AAAAAA GGAGQGGYGGLGSQGAGRGGLGGQGAG
AAAAAAA GGAGQGGYGGLGNQGAGRGGQGAG
AAAAAA GGAGQGGYGGLGSQGAGRGGLGGQGAG

P. fucata
GAGA GGGAGGGAGGGA
GAGAGAGAGAGAGAGLGLGL GGGLGGGL
.....
AAAAAAAAAAAA GGGWGGGMGGGF
GVGL GGGFGGGFGGGS

Figure 1. Amino acid sequences taken from *Antheraea pernyi*[5] and *Bombyx mori*[3,4] silk fibroin, *Nephila clavipes*[7] dragline silk spidroin 1 (MaSp1), and *Pinctada fucata*[17] insoluble protein. Characteristic repetitive motifs are underlined.

* Corresponding author. Tel/Fax: +81-42-383-7733. E-mail: asakura@cc.tuat.ac.jp.
† Tokyo University of Agriculture and Technology.
‡ Oxford Biomaterials Ltd.

10.1021/bm060155k CCC: $33.50
Published on Web 05/13/2006

Table 1. Amino Acid Sequences of Five Peptides Synthesized Here and Their Ca^{2+} Binding Assay.

sample name	amino acid sequence	conformation of the flanking Ala-Gly domain after FA treatment	Ca^{2+} concentration that bound to the film (mM, $n = 3$)
MSI60	EYDYDDDSDDDDEWDG	random coil	not determined[a]
$(A)_{12}$-MSI60	AAAAAAAAAAAAEYDYDDDSDDDDEWDAAAAAAAAAAAA	β-sheet	0.180 ± 0.010
$(AG)_6$-MSI60	AGAGAGAGAGAGEYDYDDDSDDDDEWDAGAGAGAGAGAG	random coil	0.155 ± 0.024
$(AGG)_4$-MSI60	AGGAGGAGGAGGEYDYDDDSDDDDEWDAGGAGGAGGAGG	random coil	0.105 ± 0.004
$(AGGG)_3$-MSI60	AGGGAGGGAGGGEYDYDDDSDDDDEWDAGGGAGGGAGGG	random coil	0.065 ± 0.005

[a] When dissolved in formic acid, the peptide containing only the MSI60 sequence did not form a film after air-drying.

Table 2. ^{13}C Chemical Shifts (in ppm from TMS) of the Peptides after TFA, LiBr, and FA Treatments[a]

peptides	treatment	^{13}C chemical shifts (ppm)					conformation of flanking Ala-Gly domain
		Ala C_α	Ala C_β	Ala C=O	Gly C_α	Gly C=O	
GDGG$(A)_{12}$GGAG	TFA	52.5	15.7	176.2			α-helix
	LiBr	48.5	20.0, 21.3, 22.9	171.8			β-sheet
	FA	48.7	20.3,23.0	171.9			β-sheet
$(AG)_{15}$	TFA	48.7, 51.4	16.1, 20.0	176.4	44.6	169.4, 172.3	mixture of random coil and silk II
	LiBr	50.7	16.5	176.8	43.2	169.9	silk I
	FA	48.7	16.7, 19.6, 22.2	171.8	42.4	171.8	silk II
$(AGG)_{10}$	TFA	49.9	16.7	172.2	43.2	172.2	random coil
	LiBr	48.9	17.4	174.6	41.6	171.3	3_1-helix
	FA	48.8	17.3	174.6	41.4	171.2	3_1-helix
$(AGGG)_7$	TFA	49.0	16.5, 20.8	175.3	42.4	171.6	mixture of random coil and β-sheet
	LiBr	48.8	17.8, 21.1	173.9	42.5	168.1, 171.5	mixture of distorted 3_1-helix and β-sheet
	FA	48.9	16.8, 21.3	172.3	43.7	168.5	mixture of random coil and β-sheet
$(A)_{12}$-MSI60	TFA	51.6	14.9	175.8			α-helix
	LiBr	48.3	15.5, 19.4, 22.5	171.7			silk II
	FA	49.5	20.6, 23.7	172.9			β-sheet
$(AG)_6$-MSI60	TFA	49.8	15.5	172.4	42.8	168.9	α-helix
	LiBr	49.6	16.0	172.2	42.6		random coil
	FA	49.9	17.1	173.3	43.7		mixture of random coil and 3_1-helix
$(AGG)_4$-MSI60	TFA	50.0	16.4		43.0	172.6	random coil
	LiBr	50.4	16.8		42.6	172.2	random coil
	FA	49.5	16.7		42.5	172.9	random coil
$(AGGG)_3$-MSI60	TFA	49.6	16.0		42.6	171.5	random coil
	LiBr	50.5	16.1		42.7	171.6	random coil
	FA	50.0	17.2	173.4	43.0		mixture of random coil and 3_1-helix
reference ^{13}C		50.0	16.6	175.5	42.7	171.3	random coil (from solution NMR)
chemical shift values		52.5	15.7	176.5	44.0	172.3	α-helix
of proteins with		48.7	16.7, 19.6, 22.2	171.8	42.4	169.1	silk II (β-sheet)
typical conformation		48.9	17.4	174.6	41.6	171.3	3_1-helix

[a] The chemical shifts for the amino acid residue with typical structure are also shown.

due to their insolubility in water. According to X-ray crystallography, however, these proteins seem to take predominantly β-sheet structure. In contrast, the calcium-binding domains in N-termini were reported to have high degrees of freedom.[14]

We synthesized four different synthetic peptides, each containing the calcium-binding domain of MSI60 as a central motif flanked by one of four different short peptides, each with a different repeating sequence of Ala and Gly and chosen to be characteristic of the primary sequence of four different silk fibroins with markedly different physical properties. The structures of the different Ala-Gly repeating regions of the peptides were studied by ^{13}C CP/MAS NMR and compared to those of other synthetic peptides, each with the same primary sequence but lacking the MSI60 motif. The detailed structural analyses of these peptides should provide useful information toward the development of the silk-based biomaterials containing a high-affinity calcium-binding motif.

Materials and Methods

Sample preparation. The following peptides were synthesized by the Fmoc solid-phase method: MSI60; $(A)_{12}$-MSI60; $(AG)_6$-MSI60; $(AGG)_4$-MSI60; $(AGGG)_3$-MSI60. Hereafter, the term MSI60 is used as convenient shorthand for the calcium-binding site of the MSI60 protein. The primary sequences of the synthesized peptides are shown in Table 1. For purification, the peptides were dissolved in 9 M aqueous lithium bromide (LiBr) and dialyzed (MWCO = 1000 Da, Spectra/Por) against distilled water for 4 days at 4°C. The naturally precipitated samples after dialysis were collected and freeze-dried. The lyophilized peptides were treated with trifluoroacetic acid (TFA), LiBr, or formic acid (FA) as follows: (1) dissolution in TFA followed by precipitation in diethyl ether (TFA treatment); (2) dissolution in FA followed by air-drying (FA treatment); (3) dissolution in 9 M LiBr followed by dialysis against 3 M LiBr aqueous solution (3 h), and a final dialysis against distilled water (4 days) before air drying (LiBr treatment). The treatments are known to produce consistent well-defined changes in secondary structure in silklike peptides.[15−17]

^{13}C CP/MAS NMR Spectroscopy. The ^{13}C CP/MAS NMR experiments were performed at 25 °C with a CMX Infinity 400 NMR spectrometer operating at 100.04 MHz for the ^{13}C nucleus. Each sample was placed in a cylindrical rotor and spun at a rate of 10 kHz. The number of acquisitions was 12 000, and the pulse delays were 3 s. For decoupling, 50 kHz radio frequency field strength was used with a decoupling period of 12.8 ms. A 90° pulse width of 3.2 μs with 1 ms CP contact time was employed. Phase cycling was used to minimize artifacts. ^{13}C chemical shifts were calibrated indirectly through the adamantane methyl peak observed at 28.8 ppm relative to tetramethylsilane at 0 ppm. Data are presented in Table 2.

Calcium-Binding Assay. The cast films (approximately 60 μm thick) of each peptide dissolved in formic acid were prepared by unforced evaporation at 20 °C. One cm^2 of each cast film was immersed in 100 mL of 1 mM $CaCl_2$/Tris buffer (pH 7.5) for 1 h. After removing the films from the buffer, the remaining Ca^{2+} concentration in the buffer was determined spectrophotometrically using the methylxylenol blue (MXB) method with observation at 610 nm using the V-530 type UV−vis spectrometer (JASCO co., Japan). Before measuring each sample, a calibration curve was prepared using the the calcium E-test work kit (Waco Co., Japan). Three separate results for each film were highly consistent and were averaged.

Results and Discussion

Conformation of the Calcium-Binding Domain, EYDYDDDSDDDDEWDG, Selected from the Protein MSI60. Figure 2 shows ^{13}C CP/MAS NMR spectra of EYDYDDDSDDDDEWDG (abbreviated to MSI60) and the peak assignments after the following solvent treatments: TFA (a), LiBr (b), and FA (c) treatments. The stick spectra calculated by assuming that all residues are random coil (d), α-helix (e), and β-sheet (f) are also shown. This peptide is composed of only six different amino acids (E, Y, D, S, W, and G), and more than half of the total number of amino acids (9/16) are aspartic acid (D). Thus, the conformation-dependent C_α and C_β chemical shifts of Asp residues can be used to discuss the whole conformation of the peptide. Both C_α and C_β peaks of Asp residues in the peptide are sharp after FA treatment (c), and the chemical shifts are in agreement with the random coil chemical shift within experimental error. Thus, the peptide after FA treatment takes random coil conformation.

The spectra become similar after TFA and LiBr treatments, and both peaks of C_α and C_β of Asp residues become broader. In comparison with the stick spectra, both observed spectra suggest that the main component is random coil. In addition, after TFA treatment, the peak top of the broad peak at around 35 ppm shifts to a higher field, and the peak intensity at around 53 ppm increases. In our previous reports,[10,18] silk and silklike proteins have been reported to form α-helix after TFA treatment. Thus, as noticed by comparison with the stick spectra, α-helical conformation also appears after TFA and LiBr treatments.

Conformation of the MSI60, EYDYDDDSDDDDEWD, Introduced between Different Ala-Gly Repeating Regions Taken from Silk Fibroins. Figure 3 shows ^{13}C CP/MAS NMR spectra of MSI60, $(A)_{12}$-MSI60, $(AG)_6$-MSI60, $(AGG)_4$-MSI60, and $(AGGG)_3$-MSI60 after TFA (a), LiBr (b), and FA (c) treatments. Unfortunately, Asp C_α peaks overlap with Ala C_α peaks from the flanking Ala-Gly domains, and only the Asp C_β peak can be used to investigate the conformation of the MSI60 domains introduced between different Ala-Gly repeating regions.

After TFA treatment, the Asp C_β peaks became slightly sharper for $(A)_{12}$-MSI60, $(AG)_6$-MSI60, $(AGG)_4$-MSI60, and $(AGGG)_3$-MSI6 compared with the corresponding peak in MSI60 without flanking silklike domains. This suggests that the conformation became more random. However, the peak of Asp C_β was still broad for $(A)_{12}$-MSI60 and almost the same as that of MSI60 without flanking peptides after LiBr treatment. On the other hand, the peak became sharper for $(AG)_6$-MSI60, $(AGG)_4$-MSI60, and $(AGGG)_3$-MSI6. Similarly after FA treatment, the Asp C_β peak of $(A)_{12}$-MSI60 was slightly broader than the corresponding peak of MSI60. However, FA treatment considerably sharpened the Asp C_β peak of $(AG)_6$-MSI60, $(AGG)_4$-MSI60, and $(AGGG)_3$-MSI60, suggesting the appearance of β-sheet structure.

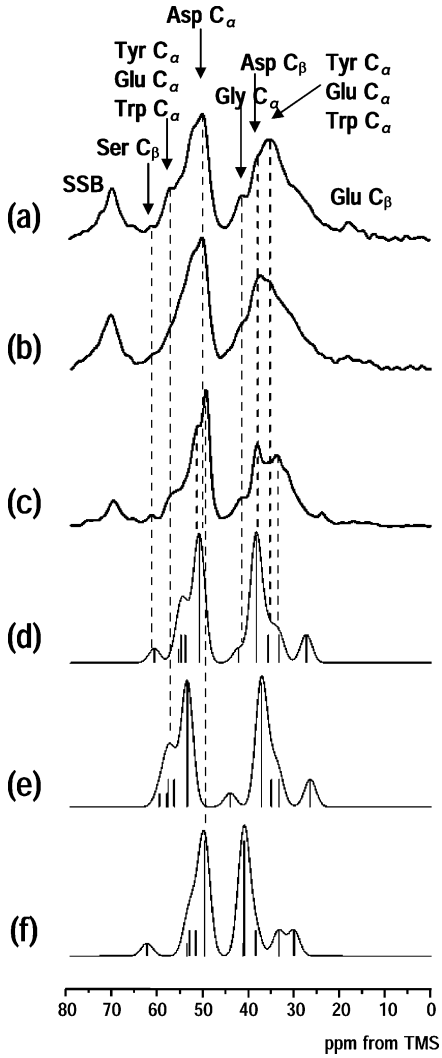

Figure 2. ^{13}C CP/MAS NMR spectra of MSI60 peptide (EYDYDDDSDDDDEWDG) after TFA treatment (a), LiBr treatment (b), and FA treatment (c). The peak assignments are included. The stick spectra were generated, taking into consideration the number of each amino acid residue in the construct and the chemical shift values of typical conformations. Thereafter, the Gaussian distribution was applied to obtain the simulated spectral curves. The stick spectra of MSI60 were calculated assuming all the residues are in a typical conformation: random coil (d), α-helix (e), and β-sheet (f). SSB indicates spinning sideband.

Structure of Flanking Ala-Gly Regions in Silklike Peptides Containing the Calcium-Binding Sequence, EYDYDDDSDDDDEWD. Since the MSI60 domain does not contain either Ala and Gly residues, the conformational information from the Ala and Gly carbon peaks can be applied to the conformational analysis of flanking Ala-Gly domains. The Ala C_β region contains a great deal of conformational information.[17,19] The conformational changes of the flanking Ala-Gly domains of the

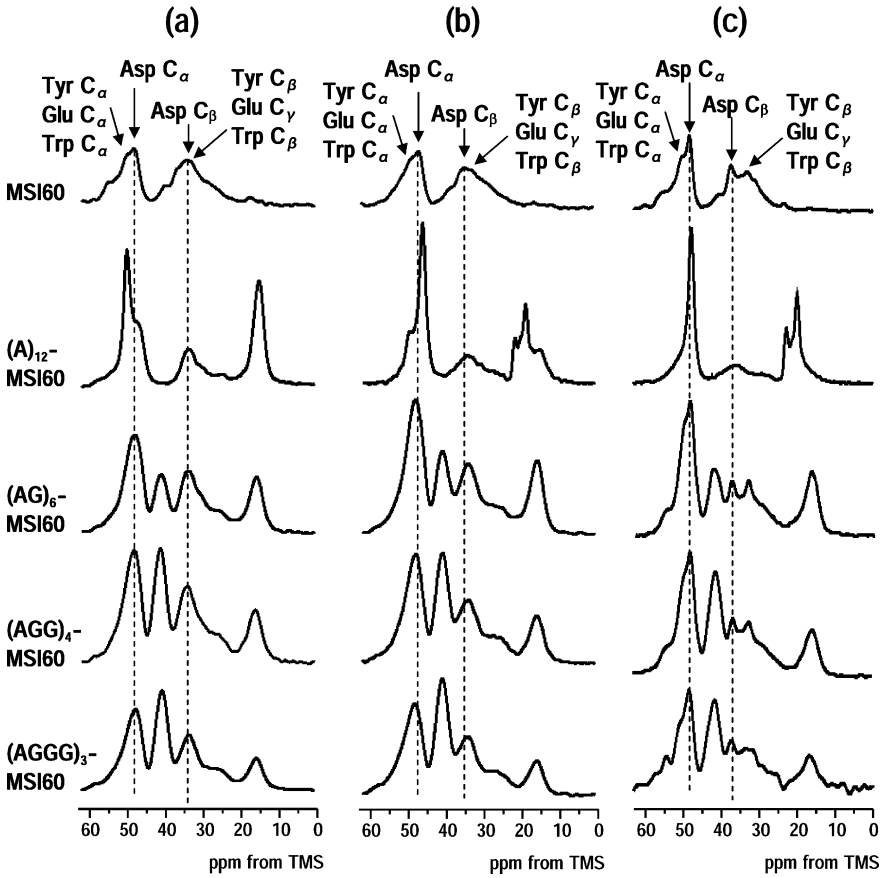

Figure 3. ^{13}C CP/MAS NMR spectra of MSI60, $(A)_{12}$-MSI60, $(AG)_6$-MSI60, $(AGG)_4$-MSI60, and $(AGGG)_3$-MSI60 peptides after TFA treatment (a), LiBr treatment (b), and FA treatment (c). The amino acid sequences of these peptides are listed in Table 1.

designed peptides can be recognized by comparing the spectra of two corresponding peptides, a peptide composed only of Ala-Gly domain, and MSI60 domains flanked by the same Ala-Gly domains. The details of the secondary structures of four silklike peptides with different repeating sequences of Ala and Gly; $GDGG(A)_{12}GGAG$, $(AG)_{15}$, $(AGG)_{10}$, and $(AGGG)_7$, after TFA, LiBr, and FA treatments have been reported in our previous papers.[10,16,18,20]

For $(A)_{12}$-MSI60 treated with TFA, the Ala C_α peak was observed at 51.6 ppm and Ala C_β at 14.9 ppm. Thus, the poly(Ala) region in the peptide $(A)_{12}$-MSI60 takes exclusively an α-helix, which is the same as the conformation of $GDGG(A)_{12}GGAG$ after the same treatment.[10,15,21] This indicates that the presence of the MSI60 domain has no influence on the inherent structure of poly(Ala) after TFA treatment. Although the peaks from Ala C_α of the peptide $(A)_{12}$-MSI60 overlap with the Asp C_α peaks from the MSI60 domain, the chemical shifts of C_α, C_β, and C═O of Ala residues show that after LiBr and FA treatments the conformations of poly(Ala) were silk II[17,19] and β-sheet, respectively. Thus, the poly(Ala) region in $(A)_{12}$-MSI60 after TFA treatment formed α-helix, and the conformation was changed from α-helix to β-sheet by LiBr and FA treatments. Therefore, the presence of MSI60 domain in $(A)_{12}$-MSI60 does not affect the conformational transition from α-helix to β-sheet in the poly(Ala) domain. Two sharp peaks were observed in the Ala C_β region for $(A)_{12}$-MSI60 after FA treatment (20.6 and 23.7 ppm), although both can be assigned to β-sheet.[22]

In comparison with $(A)_{12}$-MSI60, the spectra of $(AG)_6$-MSI60 and $(AG)_{15}$ without MSI60 showed significant differences in the (AG) repeating domains. The chemical shifts, 49.8 ppm for Ala C_α and 15.5 ppm for Ala C_β, indicate that $(AG)_6$-MSI60 takes α-helical conformation after TFA treatment. This is not the case for the molecule $(AG)_{15}$ after TFA treatment (Figure 4a, right below) in which TFA treatment increased the fraction of silk II significantly. LiBr treatment of $(AG)_6$-MSI60 gave an Ala C_α peak at 49.6 ppm, an Ala C_β peak at 16.0 ppm, and a Gly C_α peak at 42.6 ppm (Figure 4b, right upper). Comparison of the effect of LiBr treatment on the peptides $(AG)_{15}$ and $(AG)_6$-MSI60 showed that the MSI60 domain changed the conformation of the poly(AG) from silk I to random coil. After FA treatment of $(AG)_6$-MSI60, however, the main peaks of Ala C_α and C_β were observed at 49.9 and 17.1 ppm, respectively, indicating the coexistence of random coil and 3_1-helical conformation[23,24] in the peptide. When the effects of the three different solvent treatments are compared, it is clear that the MSI60 domain, which has a considerable number of hydrophilic negatively charged Asp residues, is capable of influencing the conformation of the flanking $(AG)_6$ domain after three different solvent treatments.

As shown in Figure 5 (left), the peptide $(AGG)_4$-MSI60 took random coil conformation after TFA treatment as did $(AGG)_{10}$ without MSI60 under the same conditions. The chemical shift at around 17 ppm of Ala C_β for $(AGG)_{10}$ showed that the poly(AGG) domain adopted a distorted 3_1-helix after LiBr and FA treatments. However, the Ala C_β peak shifted to 16.7 ppm and became broader for $(AGG)_4$-MSI60, quite unlike the corresponding spectrum of $(AGG)_{10}$ without MSI60 under the same condition. This indicates that, in the case of LiBr or FA treatment, the MSI60 domain in $(AGG)_4$-MSI60 is able to convert the 3_1-helix seen in the peptide $(AGG)_{10}$ to random coil.

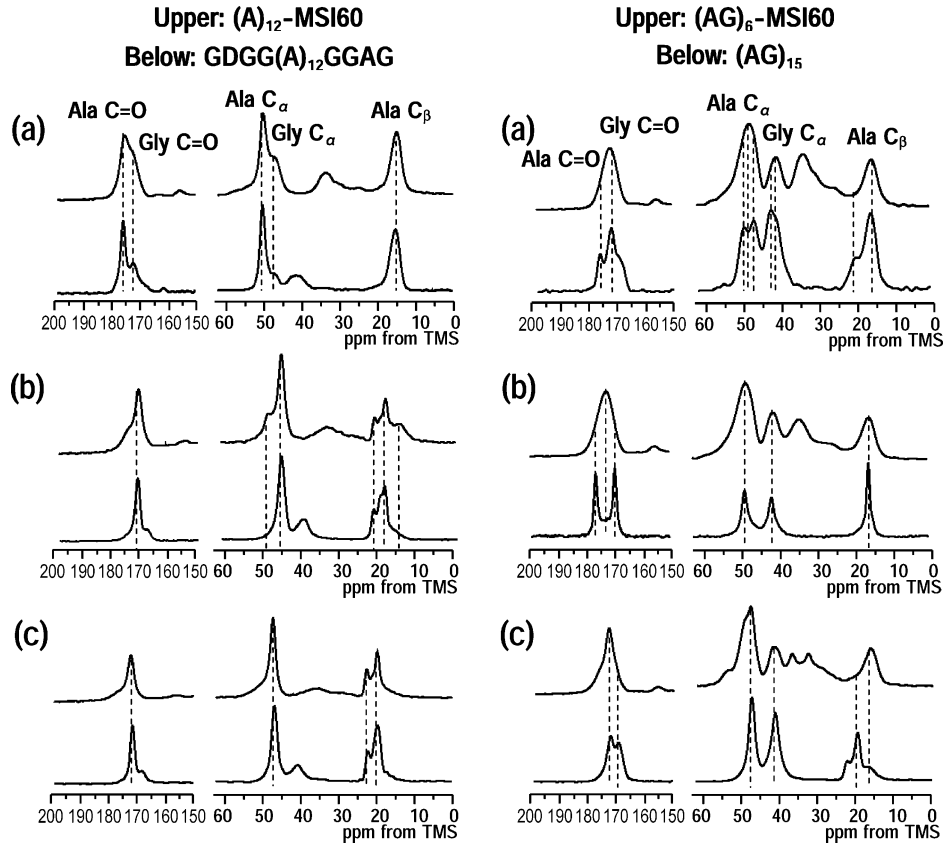

Figure 4. ^{13}C CP/MAS NMR spectra of $(A)_{12}$-MSI60 and $(AG)_6$-MSI60 peptides after TFA treatment (a), LiBr treatment (b), and FA treatment (c). The spectra of corresponding model peptide without MSI60 domains after the same treatment are shown below for comparison.

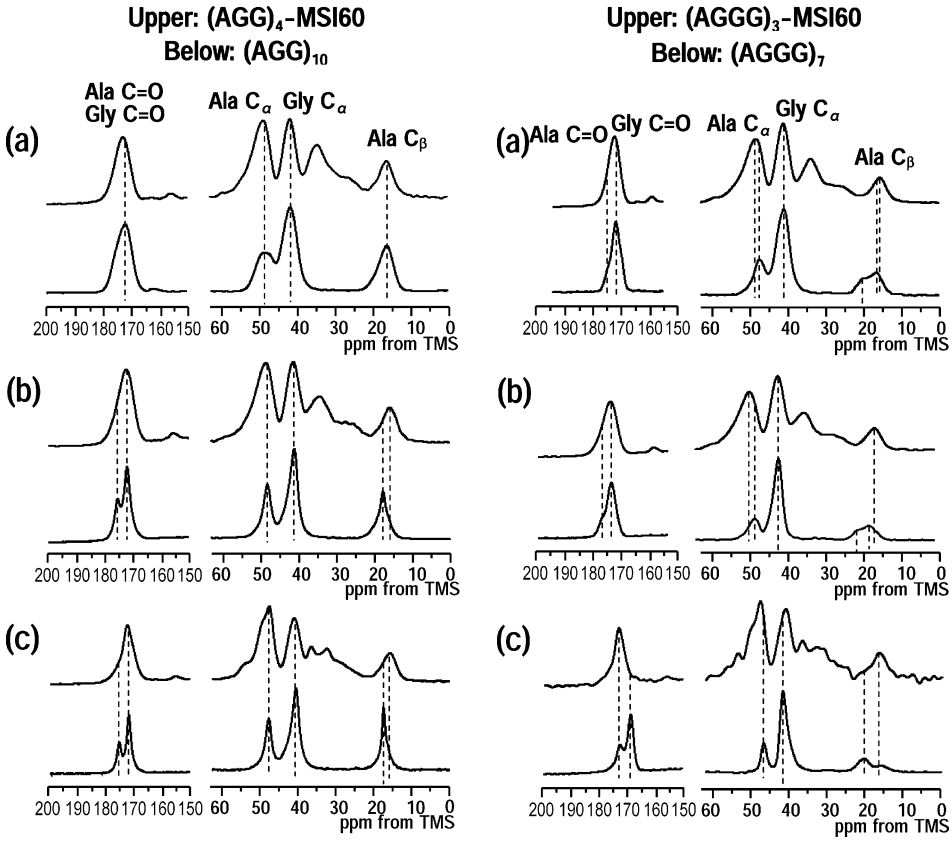

Figure 5. ^{13}C CP/MAS NMR spectra of $(AGG)_4$-MSI60 and $(AGGG)_3$-MSI60 peptides after TFA treatment (a), LiBr treatment (b), and FA treatment (c). The spectra of corresponding model peptide without MSI60 domain after the same treatment are shown below for comparison.

The conformation of $(AGGG)_3$-MSI60 (Figure 5, right) appeared to be random coil after both TFA and LiBr treatments, as the Ala C_β peaks were slightly shifted to the random coil position and were sharper compared with the corresponding

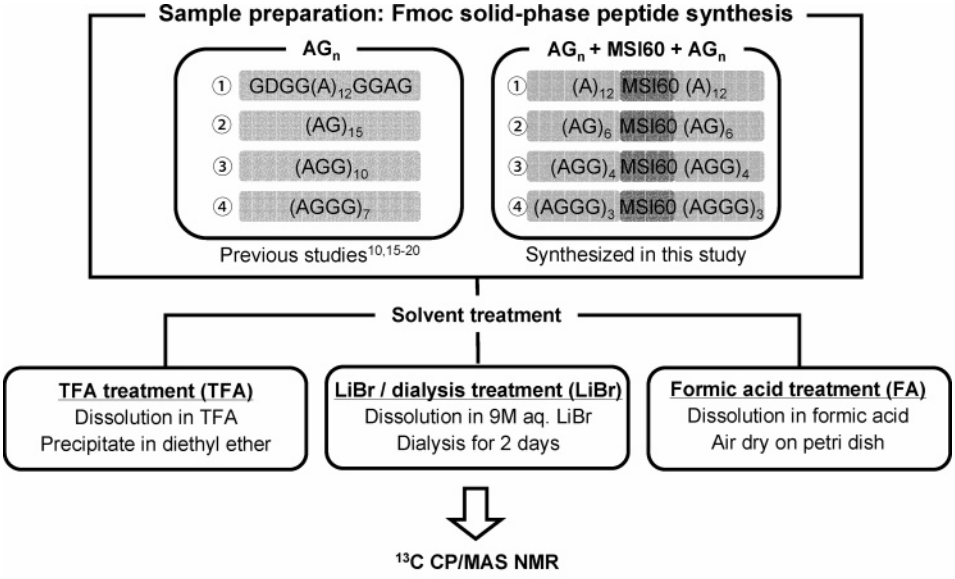

Peptides	Conformation after treatment		
	TFA	LiBr	FA
GDGG(A)$_{12}$GGAG	α-helix	β-sheet	β-sheet
(A)$_{12}$-MSI60-(A)$_{12}$	α-helix	silk II	β-sheet
(AG)$_{15}$	random coil silk II	silk I	silk II
(AG)$_6$-MSI60-(AG)$_6$	α-helix	random coil	random coil 3$_1$-helix
(AGG)$_{10}$	random coil	3$_1$-helix	3$_1$-helix
(AGG)$_4$-MSI60-(AGG)$_4$	random coil	random coil	random coil
(AGGG)$_7$	random coil β-sheet	3$_1$-helix β-sheet	random coil β-sheet
(AGGG)$_3$-MSI60-(AGGG)$_3$	random coil	random coil	random coil 3$_1$-helix

Figure 6. Flowchart illustrating the experimental procedures and the corresponding results.

spectra of $(AGGG)_7$ without MSI60. The conformation of the formal peptide after FA treatments also appeared to be a mixture of random coil and 3_1-helix in contrast to the peptide $(AGGG)_7$ without MSI60, which was predominantly β-sheet under the same conditions. Again, the presence of MSI60 domain appeared to alter the conformation of the added silklike domain after FA treatment.

In summary, the poly(Ala) domains retain the ability to undergo a conformational transition from α-helix to β-sheet in $(A)_{12}$-MSI60 despite the presence of the MSI60 domain at the center of the peptide molecule. However, the presence of this domain in the other model peptides has a marked effect on the conformation of the added silklike domains. The experimental procedures and the corresponding results are summarized in Figure 6.

Ca^{2+} Binding Assay of Silklike Peptides Containing Calcium-Binding Site from MSI60. Table 1 shows that the ability of the MSI60 domain to bind Ca^{2+} when flanked by the repetitive silk-based domains used in this study depends on their primary structure and conformation. After FA treatment of peptide films, the flanking peptides in $(A)_{12}$-MSI60 adopted a β-sheet conformation, while those in $(AG)_6$-MSI60, $(AGG)_4$-MSI60, and $(AGGG)_3$-MSI60 adopted mainly random coil as mentioned above. The ability to bind Ca^{2+} ions appeared to be the greatest when the flanking domain was in β-sheet conformation ($(A)_{12}$-MSI60 treated with FA). Interestingly, even though $(AG)_6$-MSI60, $(AGG)_4$-MSI60, and $(AGGG)_3$-MSI60 were mainly in random coil conformation, the Ca^{2+} binding ability decreased as the number of glycine residues increased. These findings suggest that the structural stability of flanking Ala-Gly sequences are important for the calcium-binding, and the presence of Gly residues with a lack of rigidity make it more difficult for MSI60 to bind Ca^{2+} ions.

Conclusions

In the present paper, we described the design of several model peptides containing silklike sequences flanking a central calcium-binding motif derived from the pearl oyster nacreous matrix protein MSI60. In the four peptides containing the MSI60 domain, the flanking silklike domains showed different secondary structures after standard treatments known to modify α-helix, β-sheet, and 3_1-helix contents in other silk proteins and silklike peptides. In addition, we observed that the amino acid residues in MSI60 had a predominantly random coil conformation after the treatments used. We also showed that the calcium-binding

capability of MSI60 domain was highest when the flanking silklike domains were in the β-sheet structure, indicating that the structural rigidity of the flanking domains advantageously affects the calcium-binding capability of the calcium-binding motif, MSI60. In addition, we have shown that poly(Ala) domains retain their ability to undergo a conformation transition from α-helix to β-sheet even when the MSI60 domain is introduced. This is likely to be important for the preparation of strong materials. These findings may provide a first step toward the development of novel protein materials combining biocompatibility, good mechanical properties, and calcium-binding capability with potential uses as implantable materials, particularly in uses such as bone graft substitutes where mineralization is important. In addition, the inclusion of MSI60 motifs in larger synthetic silklike peptides may facilitate processing into useful materials by emulating the calcium-binding sites thought to be important for the storage and natural spinning of lepidopteran fibroins.

Acknowledgment. T.A. acknowledges support from the Insect Technology Project, Japan, and Agriculture Biotechnology Project, Japan.

References and Notes

(1) Kaplan, D. L.; Adams, W. W.; Farmer, B.; Viney, C. Silk: Biology, structure, properties and genetics. In *Silk Polymers: Materials Science and Biotechnology*; Kaplan, D. L., Adams, W. W., Farmer, B., Viney, C., Eds.; ACS Symposium Series 544; American Chemical Society: Washington, DC, 1994. pp 2−16.

(2) Craig, C. L. Evolution of arthropod silks. *Annu. Rev. Entomol.* **1997**, *42*, 231−267.

(3) Suzuki, Y.; Brown, D. D. Isolation and Identification of the messenger RNA for silk fibroin from *Bombyx mori*. *J. Mol. Biol.* **1972**, *63*, 409−429.

(4) Zhou, C. Z.; Confalonieri, F.; Medina, N.; Zivanovic, Y.; Esnault, C.; Yang, T.; Jacquet, M.; Janin, J.; Duguet, M.; Perasso, R. Fine organization of *Bombyx mori* fibroin heavy chain gene. *Nucleic Acids Res.* **2000**, *28*, 2413−2419.

(5) Sezutsu, H.; Yukuhiro, K. Dynamic rearrangement within the *Antheraea pernyi* silk fibroin gene is associated with four types of repetitive units. *J. Mol. Evol.* **2000**, *51*, 329−338.

(6) Hwang, J. S.; Lee, J. S.; Goo, T. W.; Yun, E. Y.; Lee, K. S.; Kim, Y. S.; Jin, B. R.; Lee, S. M.; Kim, K. Y.; Kang, S. W.; Suh, D. S. Cloning of the fibroin gene from the oak silkworm − *Antheraea yamamai* and its complete sequence. *Biotechnol. Lett.* **2001**, *23*, 1321−1326.

(7) Hinman, M. B.; Lewis, R. V. Isolation of a clone encoding a 2nd dragline silk fibroin − *Nephila clavipes* dragline silk is a 2-protein fiber. *J. Biol. Chem.* **1992**, *267*, 19320−19324.

(8) Kong, X. D.; Cui, F. Z.; Wang, X. M.; Zhang, M.; Zhang, W. Silk fibroin regulated mineralization of hydroxyapatite nanocrystals. *J. Cryst. Growth* **2004**, *270*, 197−202.

(9) Sofia, S.; McCarthy, M. B.; Gronowicz, G.; Kaplan, D. L. Functionalized silk-based biomaterials for bone formation. *J. Biomed. Mater. Res.* **2001**, *54*, 139−148.

(10) Asakura, T.; Hamada, M.; Nakazawa, Y.; Ha, S. W.; Knight, D. P. Conformational Study of Silk-Like Peptides Containing the Calcium-Binding Sequence from Calbindin D_{9k} Using ^{13}C CP/MAS NMR Spectroscopy. *Biomacromolecules* **2006**, *7* (2), 627−634.

(11) Sudo, S.; Fujikawa, T.; Nagakura, T.; Ohkubo, T.; Sakaguchi, K.; Tanaka, M.; Nakashima, M. Structures of Mollusc Shell Framework Proteins. *Nature (London)* **1997**, *387*, 563−564.

(12) Falini, G.; Albeck, S.; Weiner, S.; Addadi, L. Control of Aragonite or Calcite Polymorphism by Mollusk Shell Macromolecules. *Science* **1996**, *271*, 67−69.

(13) Fu, G.; Valiyaveettil, S.; Wopenka, B.; Morse, D. E. $CaCO_3$ Biomineralization: Acidic 8-kDa Proteins Isolated from Aragonite Abalone Shell Nacre Can Specifically Modify Calcite Crystal Morphology. *Biomacromolecules* **2005**, *6*, 1289−1298.

(14) Weiner, S.; Traub, W. X-ray Diffraction Study of the Insoluble Organic Matrix of Mollusk Shells. *FEBS Lett.* **1980**, *111*, 311−316.

(15) Nakazawa, Y.; Asakura, T. Structure determination of a peptide model of the repeated helical domain in *Samia cynthia ricini* silk fibroin before spinning by a combination of advanced solid-state NMR methods. *J. Am. Chem. Soc.* **2003**, *125*, 7230−7237.

(16) Asakura, T.; Ashida, J.; Yamane, T.; Kameda, T.; Nakazawa, Y.; Ohgo, K.; Komatsu, K. A repeated β-turn structure in poly(Ala-Gly) as a model for silk I of *Bombyx mori* silk fibroin studied with two-dimensional spin-diffusion NMR under off magic angle spinning and retational echo double resonance. *J. Mol. Biol.* **2001**, *306*, 291−305.

(17) Asakura, T.; Yao, J. M. ^{13}C CP/MAS NMR study on structural heterogeneity in *Bombyx mori* silk fiber and their generation by stretching. *Protein Sci.* **2002**, *11*, 2706−2713.

(18) Ashida, J.; Ohgo, K.; Komatsu, K.; Kubota, A.; Asakura, T. Determination of the torsion angles of alanine and glycine residues of model compounds of spider silk $(AGG)_{10}$ using solid-state NMR methods. *J. Biomol. NMR* **2003**, *25*, 91−103.

(19) Asakura, T.; Yao, J. M.; Yamane, T.; Umemura, K.; Ulrich, K. S. Heterogeneous structure of silk fibers from *Bombyx mori* resolved by ^{13}C solid-state NMR spectroscopy. *J. Am. Chem. Soc.* **2002**, *124*, 8794−8795.

(20) Yang, M. Y.; Asakura, T. Design, expression and solid-state NMR characterization of silk-like materials constructed from sequence of spider silk, *Samia cynthia ricini* and *Bombyx mori* silk fibroins. *J. Biochem.* **2005**, *137*, 721−729.

(21) Wildman, K. A. H.; Lee, D. K.; Ramamoorthy, A. Determination of α-helix and β-sheet stability in the solid state: A solid-state investigation of poly(L-alanine). *Biopolymers* **2002**, *64*, 246−254.

(22) Asakura, T.; Okonogi, M.; Nakazawa, Y.; Yamauchi, K. Structural Analysis of Alanine Tripeptide with Anti-parallel and Parallel β-Sheet Structures in Relation to the Analysis of Mixed β-Sheet Structures in *Samia cynthia ricini* Silk Protein Fiber Using Solid State NMR. *J. Am. Chem. Soc.*, in press.

(23) Lotz, B.; Keith, H. D. The crystal structures of poly(L-Ala-Gly-Gly-Gly)II and poly(L-Ala-Gly-Gly)II. *J. Mol. Biol.* **1971**, *61*, 195−200.

(24) Wildman, K. A. H.; Wilson, E. E.; Lee, D. K.; Ramamoorthy, A. Determination of the conformation and stability of simple homo-polypeptides using solid-state NMR. *Solid State Nucl. Magn. Reson.* **2003**, *24*, 94−109.

BM060155K